Am J Transl Res 2024;16(5):2132-2146
www.ajtr.org /ISSN:1943-8141/AJTR0154472

Original Article

RACGAP1 knockdown synergizes and enhances the effects of chemotherapeutics on ovarian cancer

Jun Ye[1*], Xiang Zhang[2*], Jia-Xuan Xie[2], Yue Hou[1], Wei-Min Fan[1], Xiao-Qin Wang[1], Li-Wen Zhang[1], Xiao-Mei Yang[2], Jun Li[2], He Fei[1]

[1]Department of Obstetrics and Gynecology, The Fifth People's Hospital of Shanghai, Fudan University, Shanghai, China; [2]State Key Laboratory of Oncogenes and Related Genes, Shanghai Cancer Institute, Ren Ji Hospital, School of Medicine, Shanghai Jiao Tong University, Shanghai, China. [*]Equal contributors.

Received November 18, 2023; Accepted May 6, 2024; Epub May 15, 2024; Published May 30, 2024

Abstract: Among the three most prevalent cancers affecting the female reproductive system, ovarian cancer (OV) ranks as the second most frequently diagnosed. It is important to investigate the genomic complexity of OV to develop diagnostic and therapeutic strategies. Through the utilization of bioinformatics analysis, it was determined that RacGTPase Activating Protein 1 (RACGAP1) holds significant significance in the field of OV chemotherapeutics, an aspect that has not been thoroughly explored in prior investigations. In our study, a notable increase in RACGAP1 expression was detected in ovarian cancer, demonstrating a robust association with clinicopathological features and patient prognosis. In vivo and in vitro testing revealed that RACGAP1 acts synergistically with chemotherapeutics to enhance their effects on ovarian cancer. Furthermore, an interaction between RACGAP1 and the subunit G2 of the condensin II complex, known as non-SMC condensin II complex subunit G2 (NCAPG2), has been identified. Our findings may provide new insight for improving therapeutic strategies for OV.

Keywords: Ovarian cancer, RACGAP1, NCAPG2, chemotherapeutics

Introduction

Ovarian cancer (OV) is the second of the 3 most common cancers of the female genital system and accounts for 42.2% of all deaths [1]. Overall survival (OS) from OV has remained virtually unchanged since approximately 1980 [2]. The 10-year survival rate for patients with early-stage OV is 55%, while those diagnosed with advanced-stage disease have a significantly lower survival rate of only 15% [3]. The standardized screening approach for ovarian cancer commonly involves the utilization of both CA125 blood test and transvaginal ultrasonography. There was no significant statistical difference in survival rates observed between the group that underwent screening and the group that received standard care [4]. Carboplatin and paclitaxel constitute the universal standard regimen in the management of OV, with a response rate of approximately 65% [5]. Chemotherapy resistance is the most difficult issue in the treatment of advanced-stage OV [6]. Therefore, it is important to determine the genomic complexity of OV to develop diagnostic and therapeutic strategies [1].

RacGTPase Activating Protein 1 (RACGAP1) was first found to be involved in mammalian spermiogenesis [7]. The regulatory role of RACGAP1 has been implicated in cytokinesis [8], cell growth [9], differentiation, cell movement [10], central spindle [11] and cell cycle progression [12] based on various studies. The carcinogenic capacity of RACGAP1 has been evidenced in diverse cancer categories [13]. It is significantly overexpressed in many tumors: colorectal cancer (CRC) [14], gallbladder cancer (GBC) [9], breast cancer (BRCA) [15] and OV [16]. The high expression of RACGAP1 serves as an independent predictive marker for lymph node metastasis, recurrence, and poor prognosis in CRC [14]. The presence of RACGAP1 at the leading edge in gastric cancer is strongly correlated with factors suggesting tumor advancement and unfavorable prognosis [17]. Wang et al. discovered a

https://doi.org/10.62347/QNZU1402

significant correlation between high expression of RACGAP1 and tumor pathological grade, stage, and lymph node metastasis in OV. Patients with lower levels of RACGAP1 exhibited longer survival times and reduced recurrence risk. Cellular studies have shown that RACGAP1 can upregulate migration and invasion [16], but little is known about its exact influence on OV.

In this study, we examined data from The Cancer Genome Atlas (TCGA) and Gene Expression Omnibus (GEO) databases to investigate the involvement of RACGAP1 in the development of ovarian cancer. We conducted a comprehensive pan-cancer analysis of RACGAP1 expression across various tumor types and normal tissues, with a specific focus on ovarian cancer. Additionally, we investigated the correlation between RACGAP1 expression and clinic-pathological features, as well as evaluated its prognostic significance. Furthermore, we performed in vitro and in vivo experiments to investigate the potential impact of RACGAP1 on ovarian cancer treatment outcomes and prognosis. We employed a bioinformatic analysis software (https://bioinfogp.cnb.csic.es/tools/venny/) to identify genes that interact with RACGAP1. The collective findings of our study indicate that RACGAP1 may exert significant influence on the progression of ovarian cancer.

Methods

Bioinformatics data collection

To analyze RACGAP1 mRNA differential expression between tumor and normal tissues, we conducted a pan-cancer analysis using TCGA data through GEPIA (http://gepia.cancer-pku.cn/), with statistical significance defined as $|log2FC| > 1$ and $P < 0.01$. Subsequently, we obtained RACGAP1 gene expression and clinical information from ovarian cancer patients in The Cancer Genome Atlas (TCGA) (https://portal.gdc.cancer.gov/repository) to elucidate the clinical relevance of RACGAP1.

To mine differential expression datasets of RACGAP1-related genes, we obtained ovarian cancer microarray profiles from the GEO database (https://www.ncbi.nlm.nih.gov/gds). Three gene expression profiles, GSE6008, GSE10971, and GSE14407 were selected. Then, we evaluated RACGAP1-correlated genes through the LinkedOmics database (http://www.linkedomics.org/login.php). Meanwhile, we used Pearson correlation analysis to analyze the related genes of RACGAP1 (cor > 0.5) with GEO datasets GSE6008, GSE10971, and GSE14407.

Kaplan-Meier survival analysis

The study utilized Kaplan-Meier plotter analysis to investigate the correlation between RACGAP1 expression and both OS and progression-free survival (PFS) in ovarian cancer patients. The K-M analysis was performed in our study using the K-M plotter website (https://kmplot.com/analysis/).

Immunohistochemistry

We obtained tissue samples from ovarian cancer patients and evaluated the expression level of RACGAP1 in the tissue samples using IHC staining. First, dewaxing was performed at 65°C for 1 hour. After dewaxing, graded xylene and ethanol were used for dewaxing and hydration. Then, for antigen repair, the tissue slices were placed in boiling pH 8.0 sodium citrate buffer for 10 minutes. After cooling, the cells were incubated in hydrogen peroxide for 10 minutes. Then, the slides were sealed with 10% BSA (Sangon, Shanghai, China). The glass slide was incubated with the primary antibody against RACGAP1 (Thermo Fisher Scientific, Inc., USA) at a dilution ratio of 1:100 overnight at 4°C. The next day, the HRP secondary antibody (Thermo Fisher Scientific, Inc., USA) was allowed to incubate at room temperature for a period of 1 hour. DAB (1X) was added for approximately 5 minutes (Gene Tech, Shanghai), and the reaction was terminated in water. Ultimately, the slide underwent counterstaining using hematoxylin and was securely sealed with a neutral resin to evaluate positive areas after shooting with a scanner. When evaluating the expression level of RacGAP1 in tissues, we divided all tissues into high, medium and low expression groups based on staining intensity. Moreover, when analyzing the prognosis of patients, using only high and low expression groups can accurately analyze the effect of RacGAP1 on patient prognosis. The protocols received ethical approval from the Medical Ethics Committee of Shanghai Fifth People's Hospital, Fudan University (Ethics Review 097 in 2020).

Cell culture and reagents

The experiment utilized ovarian cancer cell lines HO-8910PM, COV318, SKOV3, OVCAR3, and HEY that were all preserved at Renji Hospital's Shanghai Cancer Institute. The cell culture was conducted using RPMI 1640 medium (provided by Beijing Solarbio Science & Technology Co., Ltd.) or F-12 medium (obtained from Gibco; Thermo Fisher Scientific, Inc.), supplemented with 10% fetal bovine serum (FBS) and 1% antibiotics (streptomycin at a concentration of 100 mg/mL and penicillin at a concentration of 100 units/mL). The cells were cultured in a temperature-controlled environment at 37°C, with a CO_2 concentration of 5% and humidity maintained. Cisplatin (CHX, MedChem Express, USA) and Taxol (CHX, MedChem Express, USA) were used in the study to treat the indicated cells.

Cell transfection

Small interfering RNA (siRNA) oligonucleotides were kindly provided by GenePharma Inc. The reduction in gene expression was accomplished by introducing small interfering RNA (siRNA) oligonucleotides into the cells, which targeted specific sequences: RACGAP1: 5'-CCCUGGACCUGUAAAGAAA-3' or 5'-GCUGAAGCAUGCACGUAAU-3'. Transfection steps were performed following the manufacturer's protocols, jetPRIME® (Polyplus transfection, France).

Real-time quantitative PCR

We set two groups to verify the efficiency of transfection: the negative control group, and the experimental group (siRACGAP1-1, and siRACGAP1-2). After a 48-hour transfection, total RNA was extracted from the cells using Trizol reagent (Thermo Fisher Scientific, Inc., USA). cDNA synthesis was performed according to the protocol of the PrimeScript™ RT Reagent Kit (Takara Bio., Inc., Otsu, Japan). We used nanodrop (Thermo Fisher Scientific, Inc., USA) to confirm that RNA and cDNA were not contaminated or degraded. Total RNA and DNA were stored at -80°C.

The real-time PCR analyses were conducted using 2*Universal SYBR Green qPCR Premix (Shanghai Share-Bio Technology Co., Ltd., China) on a 7500 Real-Time PCR system (Applied Biosystems, Foster City, CA) following the recommended thermal cycling settings: an initial cycle at 95°C for 30 seconds, followed by 40 cycles of denaturation at 95°C for 10 seconds and annealing/extension at 60°C for 30 seconds. The reaction system consisted of 20 μl, comprising 10 μl of 2*SYBR Green qPCR Premix, 0.4 μl of forward primers, 0.4 μl of reverse primers, 200 ng/20 μl CDNA, and nuclease-free water. The primers were procured from TsingkeBiotechnology Co., Ltd. The following primer sequences employed in quantitative real-time PCR were used for the detection of RacGAP1 [18]: RACGAP1-F: CTATGATGCTGAATGTGCGG, RACGAP1-R: AATCCTCAAAGTCCTTCGCC.

We employed the $2^{-\Delta\Delta}Ct$ method to calculate relative mRNA concentrations, which were normalized against GAPDH expression. The $2^{-\Delta\Delta}Ct$ value represented the disparity between the two groups for a specific target gene. The computation formula can be expressed as: 2^{-} [$^{\Delta}Ct$ = Ct (target gene) - Ct (reference gene)], and $^{\Delta\Delta}Ct$ is calculated as - [Ct (negative control group) - $^{\Delta}Ct$ (group transfected with negative control reference siRNA)].

CCK8 assay

After 48 hours of siRNA transfection, the indicated cells were counted, diluted to the required density and then placed on a 96-well plate. A volume of 100 μl containing a cell suspension with a count of 5000 cells was introduced into every well. Cells were divided into 6 groups, vehicle, vehicle+cisplatin, vehicle+Taxol, vehicle+si-RACGAP1, vehicle+si-RACGAP1 plus cisplatin, and vehicle+si-RACGAP1 plus Taxol. After the cells adhered to the surface, we removed the culture medium and added 10 μl of CCK8 reagent (Share bio, Shanghai, China) to each well. Then, we supplemented each well with 90 μl of fresh culture medium. The plate was placed in a cell incubator at 37°C for 1 hour, and the measurement of absorbance was conducted at a wavelength of 450 nm on day 0. After 24 hours, medication was added, and the drug concentration in the dosing group was equal to the IC_{50} of the corresponding cells. Then, the same method was used to measure the absorbance at 0, 1, 2, 3, and 4 days.

Subcutaneous mouse model

Five- to six-week-old female nude mice were purchased from Shanghai Slac Laboratory

Animal Co., Ltd. The use of mice was approved by the Institutional Animal Care and Use Committee (IACUC) of Songjiang District Chedun Experimental Animal Breeding Farm Co., Ltd. (IACUC approval number 2020 JS 011). The mice were taken care of very carefully. We constructed a subcutaneous implanted tumor model in nude mice. The nude mice were initially randomized into the following groups: vehicle group, vehicle+cisplatin-injection group, vehicle+Taxol-injection group, interference group, interference+cisplatin-injection group, and interference+Taxol-injection group. All mice were anesthetized using 2% isoflurane before injection to avoid pain. There were 6 mice in each group (n=6). Each mouse received a subcutaneous injection comprising 1×10^6 cells. The weekly measurements included the assessment of tumor volume and body weight in each mouse. The drugs were injected into the interior of the tumors twice a week while the subcutaneous tumor grew to 5 mm^3. According to the instructions, the administered dose of cisplatin was 25 mg/kg, while the administered dose of Taxol was 10 mg/kg. All the mice survived the presence of the subcutaneous tumor until being harvested at 5 weeks. Tumor-bearing mice were euthanized before tumor volumes exceeded 1000 mm^3 to meet the animal care principle. The mice were ultimately euthanized through cervical dislocation. After confirming the death of the mice, we used a scalpel to harvest the tumors. Because of reasonable experimental design, all mice were euthanized. The total number of samples is 36 cases. We obtained measurements for the dimensions of the tumors, including their length (L) and width (W). The studies were conducted in accordance with the Guide for the Care and Use of Laboratory Animals published by the U.S. National Institutes of Health.

TUNEL assay

We used a TUNEL assay kit (Thermo Fisher Scientific, Inc., USA) to detect apoptosis. The tissues were embedded in paraffin and sectioned to a thickness of 4 μm for the assay. The procedures of dewaxing, hydration, and antigen repair were the same as those for immunohistochemistry. The tunnel reaction mixture was prepared in the dark. We added 20 μL of the tunnel reaction mixture to each glass slide. Then we placed the slides in a wet box at 37°C for 2 hours and kept them in a dark place. The slides were washed with PBS for a total of three times, each time lasting for 5 minutes. The nucleus was stained with DAPI for 5 minutes. Additionally, the slides underwent three rounds of washing with PBS, each lasting for 5 minutes. At last, we securely enclosed the slides and imaged them using a confocal laser scanning microscope.

Western blotting

The SKOV3 cells underwent total protein extraction by utilizing a buffer (manufactured by Beyotime Institute of Biotechnology, located in Haimen, China). The BCA protein assay kit was utilized to ascertain the protein concentration. Afterwards, an equal amount of 50 μg total protein was introduced into each well for analysis. The proteins were subsequently separated using 12% SDS-PAGE and transferred onto NC membranes in equal quantities. The investigation involved the implementation of immunoblotting technique with primary antibodies specific to the target, followed by the utilization of secondary antibodies tailored for each species. The Odyssey imaging system (LI-COR Biosciences, Lincoln, NE, USA) was utilized for the detection of bound secondary antibodies. The antibodies employed in this investigation were the following: anti-RACGAP1 (rabbit, diluted at 1:1,000, Abcam Biotechnology), anti-PI3K and anti-pPI3K (rabbit, diluted at 1:1,000, Cell Signaling Technology), anti-AKT and anti-pAKT (S473) (rabbit, diluted at 1:1,000, Cell Signaling Technology), and anti-GAPDH (rabbit, diluted at 1:1,000, Sigma Biotechnology).

Co-immunoprecipitation

To conduct immunoprecipitation assays, the cells were lysed using a buffer from Beyotime (China) and then incubated with anti-RACGAP1 antibody (mouse, 1:250, Invitrogen) or species-matched IgG (Sigma)-conjugated Dynabeads® Protein A/G (Invitrogen, USA) overnight at 4°C. The beads were washed with PBS/Tween-20 for three times, after which the immunoprecipitated protein complexes were resuspended in 2× loading buffer followed by western blot analysis.

Statistical analysis

The statistical analysis was conducted using SPSS 22.0 (SPSS Inc., Chicago, IL, USA) and R

software. The software utilized for generating graphical representations was GraphPad Prism 9 (La Jolla, CA). The differences between groups were analyzed using Student's t-test. The relationships between RACGAP1 expression levels and clinicopathological factors were assessed using the Mann-Whitney U test (R function Wilcox test) and Kruskal-Wallis test (R function Kruskal test). Pearson's χ^2 test was also used to assess RACGAP1-related and coexpressed genes. We employed the Kaplan-Meier method to determine the overall survival and progression-free survival rates. We used the R package clusterProfiler to perform GSEA, GO, and KEGG enrichment analyses. All data were expressed as the mean ± standard deviation (SD). A *P* value < 0.05 was considered significant. The confidence interval is 95%.

Results

RACGAP1 expression is significantly upregulated in OV

We performed a pancancer analysis to analyze RACGAP1 mRNA differential expression between tumor/normal tissues based on TCGA data by GEPIA. In GEPIA, red text indicates significant upregulation (P < 0.01), green text indicates significant downregulation (P < 0.01), and black text indicates no significant change (P ≥ 0.01) between cancer and normal tissues. The results demonstrated a significant upregulation of RACGAP1 expression levels in OV, BRCA, esophageal carcinoma (ESCA), cervical squamous cell carcinoma (CESC), and uterine corpus endometrial carcinoma (UCEC) (**Figure 1A**).

In order to conduct a more thorough examination of RACGAP1 expression in ovarian cancer, data from a patient cohort was acquired through The Cancer Genome Atlas (TCGA) and accessed via The Genomic Data Commons (GDC) website repository. The data were obtained by utilizing the "download" function of the suggested download tool gdc-client (https://gdc.cancer.gOVCaccess-data/gdc-data-metastatic-tool). And OV-related expression data GSE6008 (consisting of 99 ovarian cancer samples and 4 non-cancer samples), GSE109-71 (consisting of 12 ovarian cancer samples and 12 non-cancer samples), and GSE1440 (consisting of 13 ovarian cancer samples and 24 non-cancer samples) were retrieved from the GEO database (https://www.ncbi.nlm.nih.gov/gds). The results demonstrated a significant upregulation of RACGAP1 in tumor tissues compared to normal tissues (**Figure 1B-E**). Then, the expression of RACGAP1 was further detected using a tissue microarray of OV (**Figure 1F** and **1G**). The expression of RACGAP1 was upregulated in 71% of OV patients (**Figure 1H**).

To assess the prognostic significance of RACGAP1, patient samples were stratified into high- and low-expression groups based on RACGAP1 mRNA levels. Utilizing the Kaplan-Meier plotter, we conducted comprehensive analyses on OS and PFS. Remarkably, elevated expression of RACGAP1 mRNA exhibited a significant association with diminished OS and PFS outcomes (**Figure 1I** and **1J**).

The mRNA expression of RACGAP1 is significantly associated with aggressive clinical characteristics in TCGA OV cancer

The TCGA database (https://tcga-data.nci.nih.gOVC/tcga/) was utilized to acquire the datasets concerning the correlation between RACGAP1 expression and clinicopathological features in patients with ovarian cancer. Based on the mRNA expression of RACGAP1, individuals were divided into two groups: those with high expression and those with low expression. We noticed a direct association between elevated RACGAP1 expression and the severity of tumors, their tendency to recur, as well as their current status. However, there was no statistically significant correlation observed between elevated RACGAP1 expression and various characteristics including age, stage, tumor lymph node infiltration and surgical debulking, etc. (**Table 1**). The data were subjected to statistical analysis using the Mann-Whitney U test (R function Wilcox test) and Kruskal-Wallis test (R function Kruskal test). A significance level of P < 0.05 was utilized to ascertain the statistical significance.

RACGAP1 knockdown enhances the effects of cisplatin or Taxol on OV cells in vitro

To investigate the role of RACGAP1 in OV, we performed Gene Ontology (GO) analysis and found that RACGAP1 expression was closely related to mismatch repair, nucleotide excision repair and drug metabolism cytochrome P450 (**Figure 2A** and **2B**). GSEA analysis showed that RACGAP1 expression was positively correlated

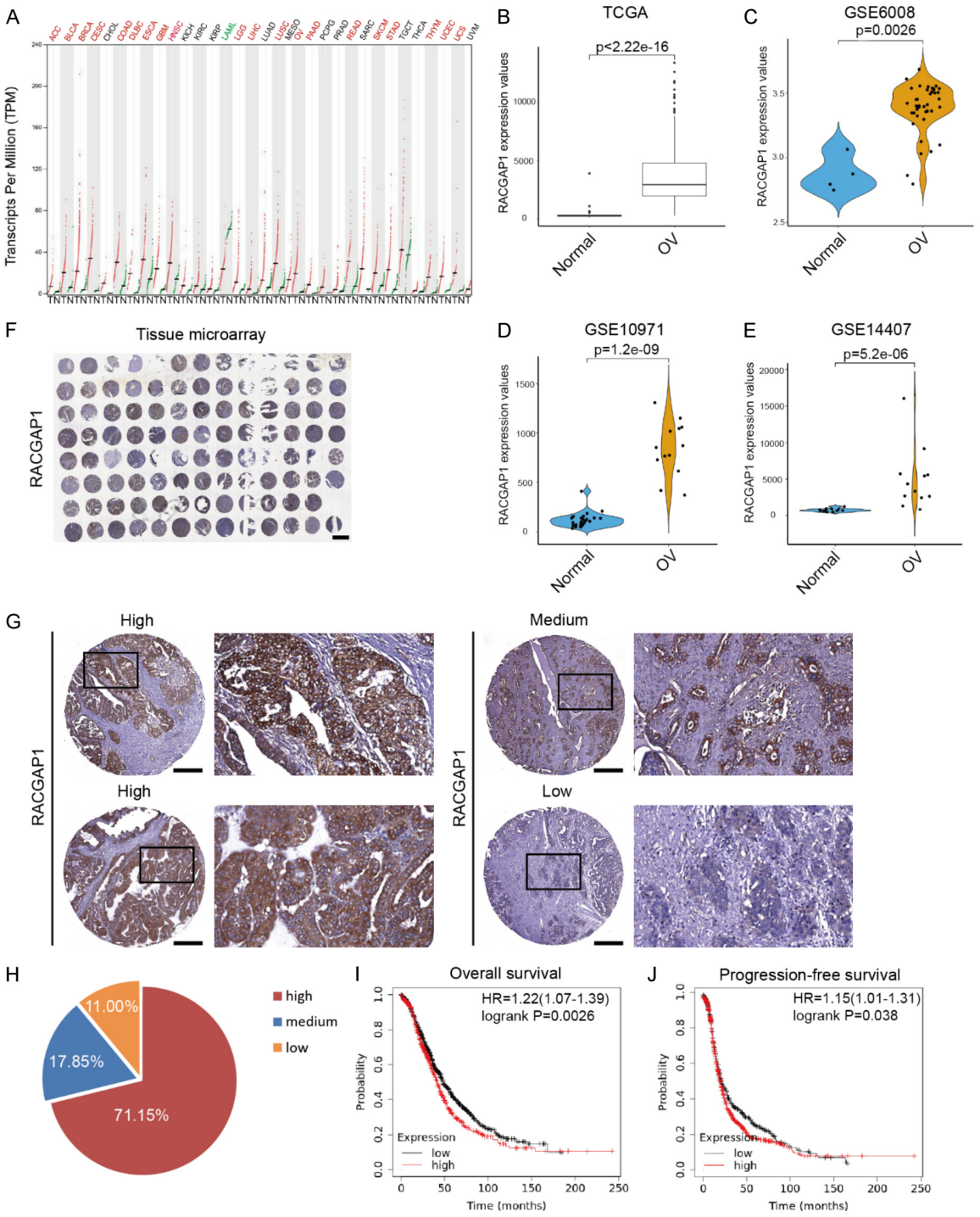

Figure 1. RACGAP1 expression is significantly upregulated in OV. (A) The comparison of RACGAP1 expression in tumor and normal tissues using TCGA data through GEPIA for a comprehensive analysis across multiple cancer types. (B-E) RACGAP1 was significantly upregulated in tumor tissues compared with normal tissues from TCGA and GEO database. (F, G) The expression of RACGAP1 was detected using a tissue microarray. (H) The expression of RACGAP1 was found to be upregulated in 71% of OV patients (high), no change in 18% of OV patients (medium) and downregulated in 11% of OV patients (low). (I, J) An increased level of RACGAP1 mRNA was observed to be significantly associated with reduced OS and PFS. Scale bar indicates 1.5 mm in (F), and 400 μm in (G). RACGAP1, RacGTPase activating protein 1; OV, ovarian cancer; OS, overall survival; PFS, progression-free survival; N, normal tissues; T, tumor tissues. The Student's t-test was employed to compare the groups, and *P* value is labeled in the graph.

Table 1. RACGAP1 mRNA expression and clinicopathological parameters in ovarian cancer patients from TCGA dataset

	Cases (n=379)	RacGAP1 expression High (n=189)	RacGAP1 expression Low (n=189)	*P*-value
Age (median)				
< 60	199 (68.5)	100 (52.9)	99 (52.1)	0.1188
≥ 60	180 (51)	89 (47.1)	91 (47.9)	
Stage (%)				0.3788
I	1 (0.3)	0 (0.0)	1 (0.5)	
II	23 (6.1)	13 (7.0)	10 (5.3)	
III	295 (78.5)	145 (77.5)	150 (79.4)	
IV	57 (15.2)	29 (15.5)	28 (14.8)	
Grade (%)				0.0166*
G1	1 (0.3)	0 (0.0)	1 (0.5)	
G2	45 (11.9)	17 (9.0)	28 (14.8)	
G3	322 (85.4)	166 (88.3)	156 (82.5)	
G4	1 (0.3)	1 (0.5)	0 (0.0)	
GB	2 (0.5)	1 (0.5)	1 (0.5)	
GX	6 (1.6)	3 (1.6)	3 (1.6)	
Surgical debulking (%)				0.7493
≤ 1 cm	171 (51.0)	82 (50.0)	89 (52)	
> 2 cm	70 (20.9)	33 (20.1)	37 (21.6)	
1-2 cm	27 (8.1)	14 (8.5)	13 (7.6)	
None	67 (20)	35 (21.3)	32 (18.7)	
First-line chemotherapy (%)				0.181
Resistant	63 (23.9)	29 (21.3)	34 (26.6)	
Sensitive	154 (58.3)	79 (58.1)	75 (58.6)	
Too early	47 (17.8)	28 (20.6)	19 (14.8)	
Tumor status (%)				0.02591*
Tumor free	85 (25.4)	51 (30.5)	34 (20.4)	
With tumor	249 (74.6)	116 (69.5)	133 (79.6)	
Primary therapy outcome (%)				0.9102
CR	206 (69.1)	114 (77.6)	92 (60.9)	
PD	27 (9.1)	12 (8.2)	15 (9.9)	
PR	43 (14.4)	12 (8.2)	31 (20.5)	
SD	22 (7.4)	9 (6.1)	13 (8.6)	
Recurrence (%)				0.01333*
No	87 (24.6)	41 (23.6)	46 (25.6)	
Yes	267 (75.4)	133 (76.4)	134 (74.4)	
Lymph node metastasis (%)				0.9122
Bilateral	255 (71.4)	125 (69.8)	130 (73.0)	
Left	56 (15.7)	28 (15.6)	28 (15.7)	
Right	46 (12.9)	26 (14.5)	20 (11.2)	
Lymphatic invasion (%)				0.1786
No	48 (32.2)	29 (36.7)	19 (27.1)	
Yes	101 (67.8)	50 (63.3)	51 (72.9)	
Vital status (%)				0.2982
Alive	147 (38.8)	81 (42.9)	66 (34.7)	
Dead	232 (61.2)	108 (57.1)	124 (65.3)	

The overexpression of RACGAP1 exhibited a significant association with the grade, recurrence, and status of tumors. RACGAP1, RacGTPase activating protein 1; OV, ovarian cancer; TCGA, The Cancer Genome Atlas; CR, complete response; PD, progressive disease; PR, partial response; SD, stable disease. Statistical examinations were conducted using the Mann-Whitney U test and Kruskal-Wallis test. The *P* value marked with * emphasized statistical significance ($P < 0.05$).

with mismatch repair and nucleotide excision repair (**Figure 2C** and **2D**), which are considered to be closely related to OV chemotherapeutics [19]. Meanwhile, RACGAP1 expression was also found to be negatively correlated with drug metabolism cytochrome P450 (CYP) (**Figure 2E**), which was reported as an important signaling molecule of drug metabolism [20]. By inhibiting the promotion of cytochrome P450 on drug metabolism in OV, CYP-mediated drug metabolism significantly impacts treatment outcomes, not only by affecting the efficacy, safety, and availability of drugs but also by contributing to the development of drug resistance [21]. For instance, CYP1B1, a constituent of the cytochrome P450 enzyme group, plays a role in the development of drug resistance to docetaxel in ovarian cancer [22].

Then, we examined the impact of RACGAP1 on the responsiveness of OV cells towards cisplatin and Taxol, the most commonly used OV chemotherapy drugs. The expression level of RACGAP1 was first detected in SKOV3, HEY, C0V318, HO-8910PM, and OVCAR3 cell lines (**Figure 2F**). RACGAP1 was found to have a relatively high expression level in SKOV3 and HO-8910PM cells. Then, SKOV3 and HO-8910PM cells were selected, and RACGAP1 was knocked down using siRNA. The interference efficiency was detected by real-time PCR analysis. The interference efficiency of si-RACGAP1-1 and si-RACGAP1-2 in SKOV3 cells was 79.11% and 75.27%, respectively. The interference efficiency of si-RACGAP1-1 and si-RACGAP1-2 in HO-8910PM cells was 76.02% and 71.94%, respectively (**Figure 2G**).

Then, cisplatin or Taxol was used to treat SKOV3 and HO-8910PM cells transfected with si-NC or si-RACGAP1 (si-RACGAP1-1 plus si-RACGAP1-2). A CCK8 assay was performed to detect cell viability at 0 d, 1 d, 2 d, 3 d and 4 d. The proliferation of SKOV3 or HO-8910PM cells was suppressed in the vehicle plus cisplatin or Taxol groups. Knockdown of RACGAP1 further enhanced the effects of cisplatin or Taxol on OV cells (**Figure 2H-K**).

Knockdown of RACGAP1 enhances the effects of cisplatin or Taxol on OV in vivo

We conducted additional research to examine how RACGAP1 influences the response of OV cells to cisplatin or Taxol in a mouse model with subcutaneous implantation of SKOV3 and HO-8910PM cells transfected with sh-NC or sh-RACGAP1 (**Figure 3A**). After the mice were anesthetized, the tumor nodules were obtained. Cisplatin or Taxol administration suppressed the growth of tumor nodules. RACGAP1 knockdown further synergized and enhanced the inhibitory effects of cisplatin or Taxol on OV (**Figure 3B** and **3C**).

After detection of Ki67 and TUNEL staining, we further found that RACGAP1 knockdown could enhance the inhibitory effects of cisplatin or Taxol on the proliferation of OV cells. Meanwhile, the apoptosis of OV cells in the si-RACGAP1 plus cisplatin or Taxol-administered group was found to be increased (**Figure 3D-G**).

RACGAP1 interacts with NCAPG2 and regulates PI3K/AKT pathway in cisplatin treated ovarian cancer cells

First, we downloaded OV patient cohort data obtained from TCGA in the LinkedOmics online database (http://linkedomics.org), which was used to explore RACGAP1-related genes. The results are shown in **Figure 4A**. Meanwhile, the GEO datasets GSE6008, GSE10971, and GSE14407 were also used for Pearson correlation analysis to obtain the related genes of RACGAP1 (cor > 0.5). The results are shown in **Figure 4B**. Finally, the Venn tool was adopted to screen the overlapping genes among these genes. As a result, we found that non-SMC condensin II complex subunit G2 (NCAPG2) was the overlapped co-expressing gene of RACGAP1 in all these datasets (**Figure 4C**). As shown in **Figure 4D**, NCAPG2 expression was highly associated with RACGAP1 expression. By qPCR analyses, we found that NCAPG2 was closely related to RACGAP1 in OV tissue (**Figure 4E**). NCAPG2 was readily coimmunoprecipitated with RACGAP1 in cancer cells, and vice versa (**Figure 4F**). By using a Kaplan-Meier plotter, we observed a significant correlation between elevated levels of NCAPG2 mRNA expression and decreased OS and PFS in the TCGA database (**Figure 4G** and **4H**).

The PI3K/AKT signaling pathway plays a crucial role in modulating the sensitivity of tumor cells to cisplatin treatment [37], so we further investigated whether RACGAP1 affects the chemotherapy response of OV cells through regulating PI3K/AKT pathway. We detected the p-PI3K

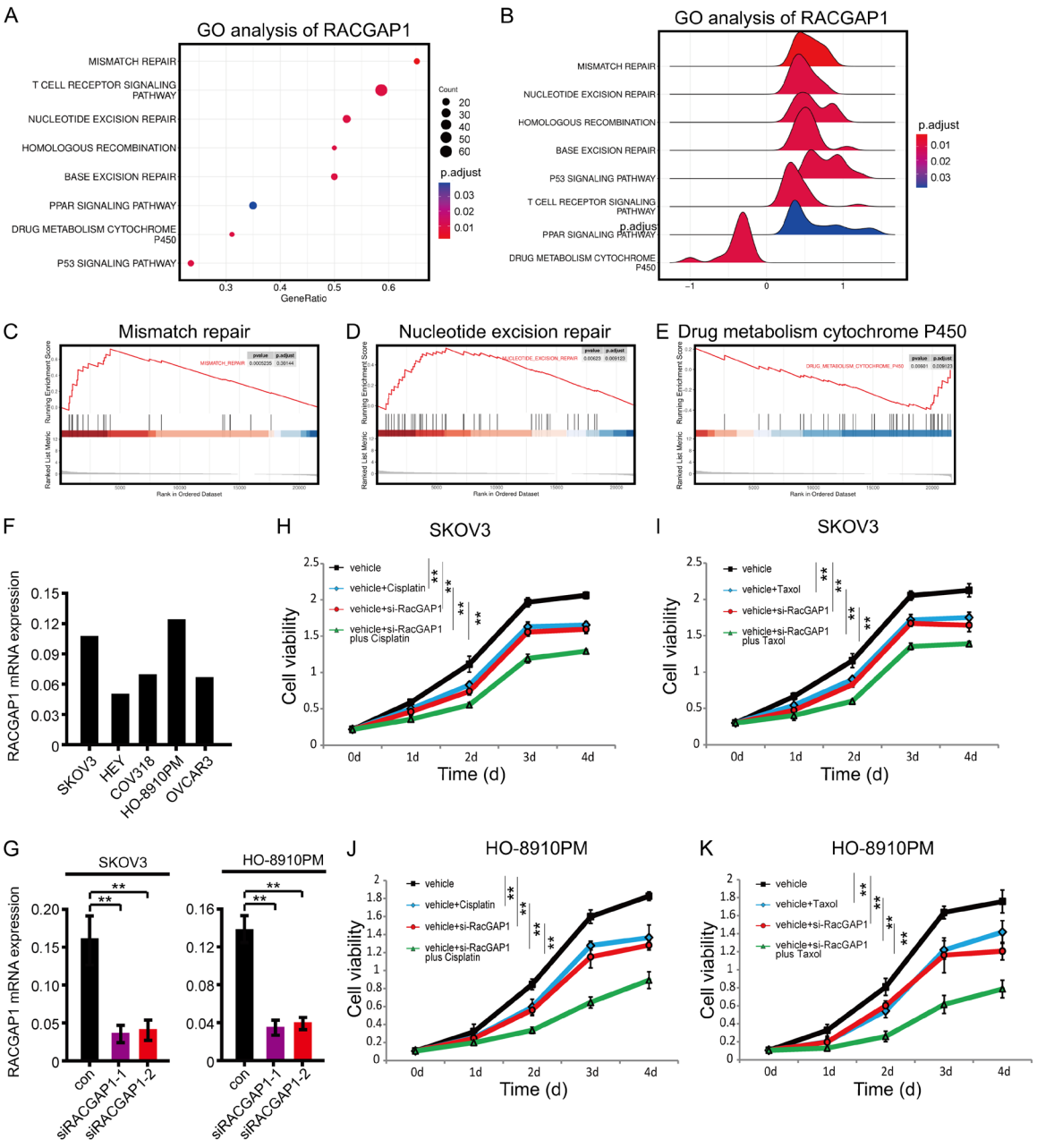

Figure 2. RACGAP1 knockdown could enhance the cytotoxic effects of cisplatin or Taxol on OV cells in vitro. (A, B) RACGAP1 expression was closely related to mismatch repair, nucleotide excision repair, and drug metabolism cytochrome P450 by GO analysis. (C-E) The GSEA analysis revealed a significant positive association between the expression of RACGAP1 and the signals generated by chemotherapeutic agents used in ovarian cancer treatment. (F) The initial assessment of RACGAP1 expression was conducted in SKOV3, HEY, COV318, HO-8910PM, and OVCAR3 cell lines. The y-axis in (F) illustrates the comparative mRNA expression level of RACGAP1 across different OV cell lines. (G) The interference efficiency of RACGAP1 in SKOV3 and HO-8910PM was detected by real-time PCR. The y-axis in (G) represents the mRNA expression level of RACGAP1 after transfection by siRNA. All the values were normalized to GAPDH. (H-K) Cells were divided into 6 groups: vehicle, vehicle+cisplatin, vehicle+Taxol, vehicle+si-RACGAP1, vehicle+si-RACGAP1 plus cisplatin, and vehicle+si-RACGAP1 plus Taxol. Cell viability of each group was measured at 0, 1, 2, 3, and 4 days. It was indicated that Knockdown of RACGAP1 further enhanced the effects of cisplatin or Taxol on OV cells analyzed by CCK8 assay. RACGAP1, RacGTPase activating protein 1; OV, ovarian cancer; GO, Gene Ontology; GSEA, Gene Set Enrichment Analysis. We employed the Student's t test to compare groups, with a significance threshold of $P < 0.01$. Significance levels were indicated as $^{**}P < 0.01$.

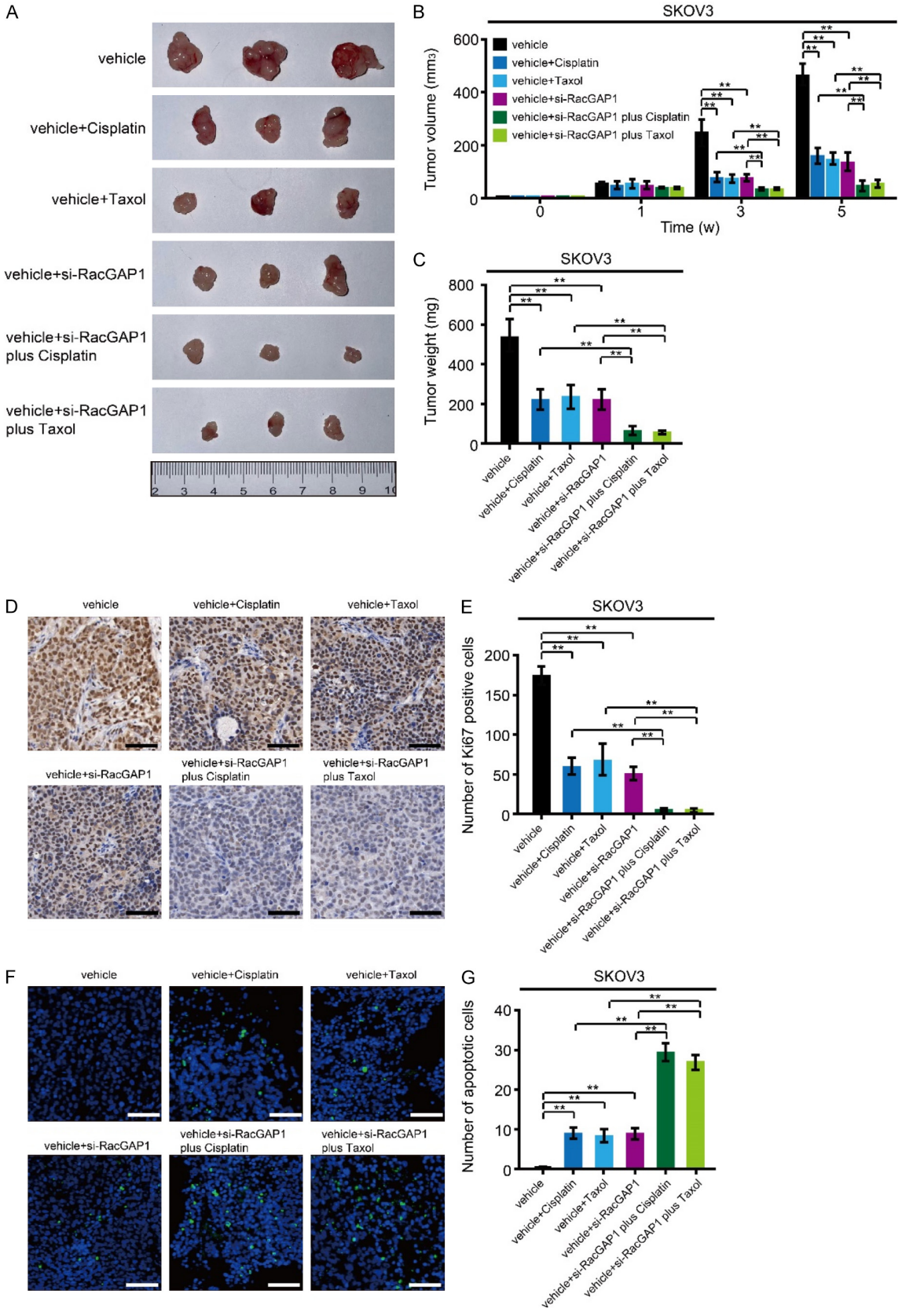

Figure 3. Knockdown of RACGAP1 enhances the effects of cisplatin or Taxol on OV in vivo. A. SKOV3 and HO-8910PM cells transfected with sh-NC or sh-RACGAP1 were subcutaneously inoculated into nude mice. The nude mice were

divided into 6 groups (n=6 in each group). The drugs were injected twice a week while the subcutaneous tumor grew to 5 mm^3. The dosage of cisplatin given was 25 mg per kilogram, while the dosage of Taxol administered was 10 mg per kilogram. Tumors were harvested and measured in the fifth week. B, C. Tumor volume was measured at 0, 1, 3 and 5 week, respectively. Comparing the tumor volume of these groups, it was known that RACGAP1 knockdown further synergized and enhanced the inhibitory effects of cisplatin or Taxol on OV. D, E. RACGAP1 knockdown could enhance the inhibitory effects of cisplatin or Taxol on the proliferation of OV cells by Ki67 staining. F, G. Reducing the expression of RACGAP1 could enhance the apoptotic effects of cisplatin or Taxol on OV cells, as evidenced by TUNEL staining. Scale bar indicates 100 μm. RACGAP1, RacGTPase activating protein 1; OV, ovarian cancer. We employed the Student's t test to compare groups, with a significance threshold of $P < 0.01$. Significance levels were indicated as $^{**}P < 0.01$.

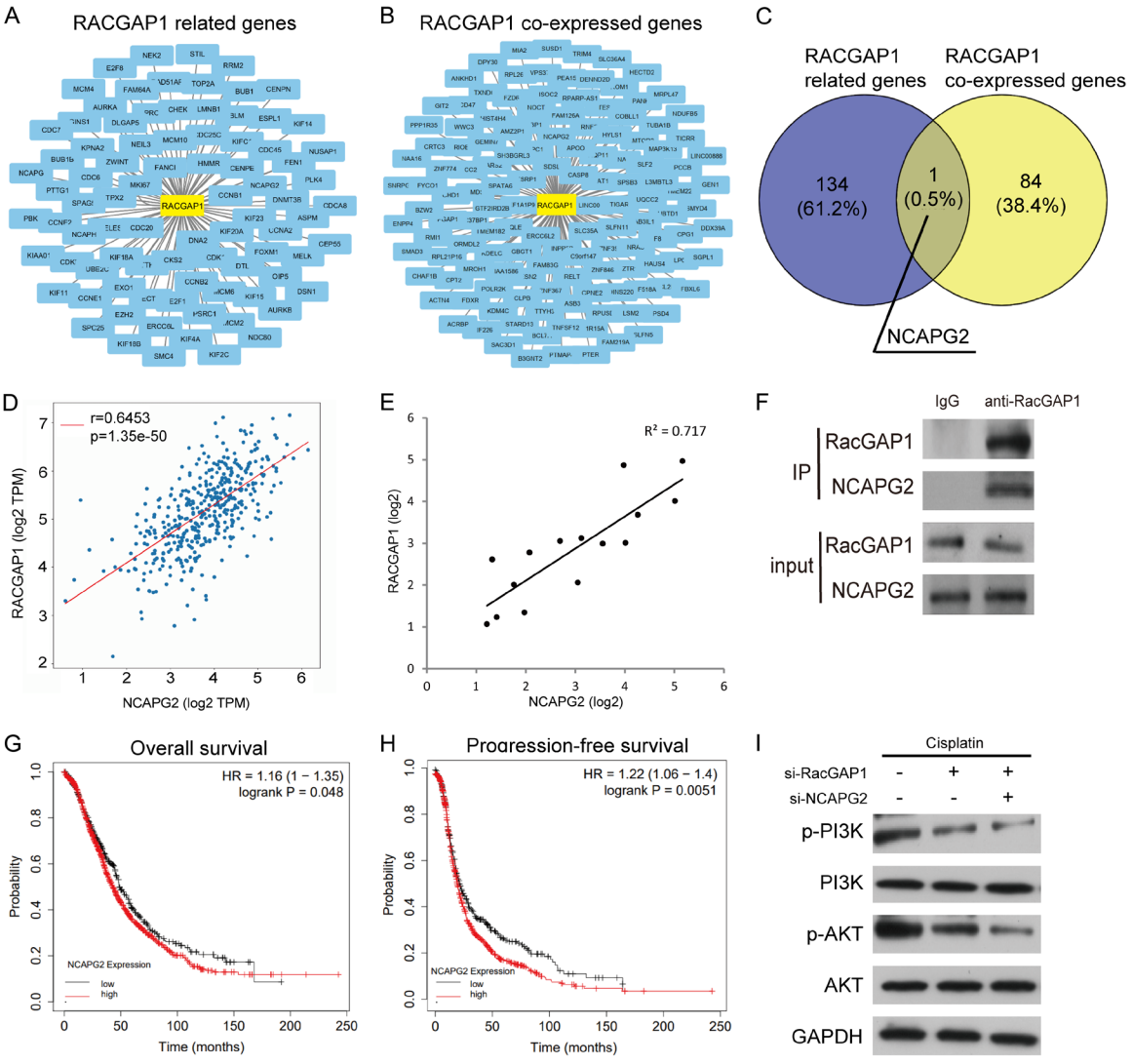

Figure 4. RACGAP1 interacts with NCAPG2 and regulates PI3K/AKT pathway in cisplatin treated ovarian cancer cells. A. OV patient cohort data obtained from TCGA in the LinkedOmics online database were used to explore RACGAP1-related genes. B. The GEO datasets were used for Pearson correlation analysis to obtain the related genes of RACGAP1 (cor > 0.5). C. NCAPG2 was co-expressed by the Venn tool. D. NCAPG2 may be closely related to RACGAP1 in OV progression. E, F. NCAPG2 is closely related to RACGAP1 in OV tissue detected by qPCR and CO-IP. G, H. The expression of NCAPG2 mRNA was found to be significantly correlated with decreased OS and PFS, as demonstrated by the Kaplan-Meier plotter analysis. I. Double knockout of RACGAP1 and NCAPG2 caused pPI3K and pAKT expression decreased significantly with cisplatin treatment. RACGAP1, RacGTPase activating protein 1; OV, ovarian cancer; NCAPG2, non-SMC condensin II complex subunit G2; OS, overall survival; PFS, progression-free survival. The Student's t-test was employed to compare the groups, and *P* value is labeled in the graph.

and p-AKT level after RACGAP1 knockdown by cisplatin treatment in SKOV3 cells. The results showed that phosphorylated PI3K and AKT were clearly downregulated by RACGAP1 knockdown, which were further suppressed by double knockout of RACGAP1 and NCAPG2 (**Figure 4I**). Therefore, the interaction between RACGAP1 and NCPAG2 may play important roles in OV chemotherapeutic resistance.

Discussion

OV is commonly detected in advanced stages and lacks an efficient screening approach. In recent years, various therapies, including traditional chemotherapy and targeted drug therapy, have been rapidly developed for late-stage OV patients [6]. Drugs targeting driver genes show a more potent anticancer effect and lower toxicity than conventional chemotherapy [23]. In advanced OV, targeted treatment plays an increasingly important role [24]. However, despite efforts to improve patient outcomes, the 5-year survival rate remains unchanged for advanced OV [5]. Furthermore, our knowledge of the underlying cellular and molecular pathways inducing therapy failure is rather limited. To solve this problem, more research is needed to explore an effective strategy covering relative cancer-promoting mechanisms and genomic complexity. Hence, the identification of more precise and dependable biomarkers for the detection and prediction of OV becomes crucial.

Bioinformatics has emerged as a highly effective instrument for conducting diverse genomics and proteomics investigations in the field of tumor research. Using pancancer analysis through GEPIA by mining RNA-seq data from the TCGA database, the results showed that the mRNA level of RACGAP1 was significantly upregulated in many human cancers compared with nontumor tissues, including OV. RACGAP1 has been identified as an oncogene. In hepatocellular-cancer (HCC), RACGAP1 overexpression could serve as an independent prognostic factor for recurrent HCC [25]. Therefore, we performed an examination on openly accessible TCGA datasets to explore the association between the mRNA expression of RACGAP1 and the clinical information of individuals diagnosed with ovarian cancer. The findings indicated a direct association between elevated levels of RACGAP1 expression and tumor grade, as well as an increased likelihood of tumor recurrence and progression.

Furthermore, we conducted a prognostic analysis of RACGAP1 by categorizing patient samples into two groups based on the level of RACGAP1 mRNA expression in the OV tissue microarray. Through the Kaplan-Meier plotter, we performed OS analyses and PFS analyses. Noticeable correlations were found between elevated mRNA expression levels of RACGAP1 and reduced OS as well as PFS. The same results were obtained in cervical cancer [26]. The results showed that RACGAP1 has potential diagnostic and prognostic value in OV, which was consistent with the finding of Wang's research [16].

RACGAP1 is a well-documented modulator of cytokinesis, migration, and differentiation [27]. Specific blockage of circRACGAP1 can enhance the therapeutic effect of apatinib in human advanced gastric cancer and reduce its toxicities [28]. CircASXL1 facilitates the proliferation, migration, and invasion of ovarian cancer cells by regulating the miR-320d/RACGAP1 signaling pathway [29]. However, we were interested in investigating the impact of elevated levels of RACGAP1 on the effectiveness of chemotherapy for ovarian cancer. Through both in vivo and in vitro experiments, it was observed that the downregulation of RACGAP1 could potentially augment the efficacy of cisplatin or Taxol against OV. These experiments demonstrate the role of RACGAP1 knockdown in enhancing clinical chemotherapy drug sensitivity in OV.

We used different bioinformatics analysis methods to analyze TCGA and GEO databases and obtained two datasets that included 135 RACGAP1 coexpressed genes and 87 RACGAP1-related genes. In the Venn diagram, we found that NCAPG2 was the only overlapping gene in the two datasets. NCAPG2 plays a critical role in the complex responsible for condensing and segregating chromosomes during mitosis, repairing DNA, and modulating histones [30]. It is frequently upregulated in many tumors [31]. NCAPG2 can interact with Polo-like kinase 1 (PLK1) during the anterior-to-metaphase transition of mitosis, thereby regulating correct chromosome segregation [32]. NCAPG2 possesses the capacity to regulate cellular proliferation through modulation of protein expression linked to the G2/M phase of

cell division [33]. Overexpression of NCAPG2 promotes HCC proliferation, migration, and invasion [34]. Phosphorylation-induced activation of HBO1 by NCAPG2 promotes the aggressiveness of glioblastoma cells and enhances xenograft tumor growth [35]. Increased NCAPG2 expression has been associated with poorer prognosis and resistance to chemotherapy [36]. For example NCAPG2 promoted erlotinib resistance by maintaining the stemness in lung adenocarcinoma [37].

In our study, the bioinformatics analysis identified a significant increase in the mRNA expression of NCAPG2 in ovarian cancer. Furthermore, it was observed that elevated expression of NCAPG2 mRNA correlated with unfavorable DFS and OS outcomes when compared to cases with lower NCAPG2 expression. A recent study suggested that NCAPG2 may modulate RACGAP1-mediated contractile ring formation, contributing to proper cell division [38].

The regulation of diverse pathophysiological processes, including cell proliferation, migration, and drug resistance, particularly in relation to cisplatin resistance, can be significantly enhanced by inhibiting the PI3K/AKT signaling pathway [39]. Hence, we investigated the impact of RACGAP1 on the effectiveness of cisplatin in ovarian cancer by examining its influence on the PI3K/AKT pathway. The findings indicate that the suppression of RACGAP1 can effectively impede the phosphorylation of PI3K/AKT. After conducting bioinformatics analysis, we observed a significant correlation between RACGAP1 and NCAPG2. Furthermore, our co-immunoprecipitation experiments confirmed their physical interaction. Meanwhile, simultaneous inhibition of both genes inhibited the phosphorylation of PI3K/AKT more than RACGAP1 single knockdown in cisplatin treated OV cells. These results suggested that the two proteins were involved in the OV chemoresistance through regulating the PI3K/AKT pathway. Disruption of RACGAP1 or NCAPG2 might improve chemosensitivity in clinical application. However, the specific mechanism by which RACGAP1 and NCAPG2 regulate the PI3K/AKT pathway in relation to cisplatin resistance remains unclear and requires further investigation in future studies.

In conclusion, RACGAP1 was found to be upregulated in OV and closely related to clinicopathological features and patient prognoses. RACGAP1 knockdown could synergize and enhance the effects of chemotherapeutics on OV. The interaction between RACGAP1 and NCPAG2 may play important roles in OV chemotherapeutics.

Acknowledgements

The current research received grants from the Natural Science Foundation in Minhang, Shanghai (No. 2020MHZ054) and High-level Professional Physician Training Program of Minhang District (No. 2020MZYS14).

Disclosure of conflict of interest

None.

Address correspondence to: He Fei, Department of Obstetrics and Gynecology, The Fifth People's Hospital of Shanghai, Fudan University, No. 801 Heqing Road, Minhang District, Shanghai 200240, China. E-mail: feihe@5thhospital.com; Jun Li, State Key Laboratory of Oncogenes and Related Genes, Shanghai Cancer Institute, Ren Ji Hospital, School of Medicine, Shanghai Jiao Tong University, No. 801 Dongchuan Road, Minhang District, Shanghai 200240, China. E-mail: junli@shsci.org

References

[1] Siegel RL, Miller KD and Jemal A. Cancer statistics, 2019. CA Cancer J Clin 2019; 69: 7-34.

[2] Vaughan S, Coward JI, Bast RC Jr, Berchuck A, Berek JS, Brenton JD, Coukos G, Crum CC, Drapkin R, Etemadmoghadam D, Friedlander M, Gabra H, Kaye SB, Lord CJ, Lengyel E, Levine DA, McNeish IA, Menon U, Mills GB, Nephew KP, Oza AM, Sood AK, Stronach EA, Walczak H, Bowtell DD and Balkwill FR. Rethinking ovarian cancer: recommendations for improving outcomes. Nat Rev Cancer 2011; 11: 719-725.

[3] Narod S. Can advanced-stage ovarian cancer be cured? Nat Rev Clin Oncol 2016; 13: 255-261.

[4] Buys SS, Partridge E, Black A, Johnson CC, Lamerato L, Isaacs C, Reding DJ, Greenlee RT, Yokochi LA, Kessel B, Crawford ED, Church TR, Andriole GL, Weissfeld JL, Fouad MN, Chia D, O'Brien B, Ragard LR, Clapp JD, Rathmell JM, Riley TL, Hartge P, Pinsky PF, Zhu CS, Izmirlian G, Kramer BS, Miller AB, Xu JL, Prorok PC, Gohagan JK and Berg CD; PLCO Project Team. Effect of screening on ovarian cancer mortality: the Prostate, Lung, Colorectal and Ovarian

(PLCO) cancer screening randomized controlled trial. JAMA 2011; 305: 2295-2303.
[5] Ozols RF. Paclitaxel (Taxol)/carboplatin combination chemotherapy in the treatment of advanced ovarian cancer. Semin Oncol 2000; 27 Suppl 7: 3-7.
[6] Matulonis UA, Sood AK, Fallowfield L, Howitt BE, Sehouli J and Karlan BY. Ovarian cancer. Nat Rev Dis Primers 2016; 2: 16061.
[7] Lin YH, Ke CC, Wang YY, Chen MF, Chen TM, Ku WC, Chiang HS and Yeh CH. RAB10 interacts with the male germ cell-specific GTPase-activating protein during mammalian spermiogenesis. Int J Mol Sci 2017; 18: 97.
[8] Warga RM, Wicklund A, Webster SE and Kane DA. Progressive loss of RacGAP1/ogre activity has sequential effects on cytokinesis and zebrafish development. Dev Biol 2016; 418: 307-322.
[9] Bian R, Dang W, Song X, Liu L, Jiang C, Yang Y, Li Y, Li L, Li X, Hu Y, Bao R and Liu Y. Rac GTPase activating protein 1 promotes gallbladder cancer via binding DNA ligase 3 to reduce apoptosis. Int J Biol Sci 2021; 17: 2167-2180.
[10] Yin H, Zhang C, Wei Z, He W, Xu N, Xu Y, Li T, Ren K, Kuang Y, Zhu X, Yuan F, Yu H and Gou X. EGF-induced nuclear translocation of SHCBP1 promotes bladder cancer progression through inhibiting RACGAP1-mediated RAC1 inactivation. Cell Death Dis 2022; 13: 39.
[11] Kamijo K, Ohara N, Abe M, Uchimura T, Hosoya H, Lee JS and Miki T. Dissecting the role of Rho-mediated signaling in contractile ring formation. Mol Biol Cell 2006; 17: 43-55.
[12] Nishimura K, Oki T, Kitaura J, Kuninaka S, Saya H, Sakaue-Sawano A, Miyawaki A and Kitamura T. APC(CDH1) targets MgcRacGAP for destruction in the late M phase. PLoS One 2013; 8: e63001.
[13] Lawson CD, Fan C, Mitin N, Baker NM, George SD, Graham DM, Perou CM, Burridge K, Der CJ and Rossman KL. Rho GTPase transcriptome analysis reveals oncogenic roles for Rho GTPase-activating proteins in basal-like breast cancers. Cancer Res 2016; 76: 3826-3837.
[14] Imaoka H, Toiyama Y, Saigusa S, Kawamura M, Kawamoto A, Okugawa Y, Hiro J, Tanaka K, Inoue Y, Mohri Y and Kusunoki M. RacGAP1 expression, increasing tumor malignant potential, as a predictive biomarker for lymph node metastasis and poor prognosis in colorectal cancer. Carcinogenesis 2015; 36: 346-354.
[15] Ren K, Zhou D, Wang M, Li E, Hou C, Su Y, Zou Q, Zhou P and Liu X. RACGAP1 modulates ECT2-dependent mitochondrial quality control to drive breast cancer metastasis. Exp Cell Res 2021; 400: 112493.
[16] Wang C, Wang W, Liu Y, Yong M, Yang Y and Zhou H. Rac GTPase activating protein 1 promotes oncogenic progression of epithelial ovarian cancer. Cancer Sci 2018; 109: 84-93.
[17] Saigusa S, Tanaka K, Mohri Y, Ohi M, Shimura T, Kitajima T, Kondo S, Okugawa Y, Toiyama Y, Inoue Y and Kusunoki M. Clinical significance of RacGAP1 expression at the invasive front of gastric cancer. Gastric Cancer 2015; 18: 84-92.
[18] Yang XM, Cao XY, He P, Li J, Feng MX, Zhang YL, Zhang XL, Wang YH, Yang Q, Zhu L, Nie HZ, Jiang SH, Tian GA, Zhang XX, Liu Q, Ji J, Zhu X, Xia Q and Zhang ZG. Overexpression of Rac GTPase activating protein 1 contributes to proliferation of cancer cells by reducing hippo signaling to promote cytokinesis. Gastroenterology 2018; 155: 1233-1249, e1222.
[19] Tomasova K, Cumova A, Seborova K, Horak J, Koucka K, Vodickova L, Vaclavikova R and Vodicka P. DNA repair and ovarian carcinogenesis: impact on risk, prognosis and therapy outcome. Cancers (Basel) 2020; 12: 1713.
[20] Janssen EM, Dy SM, Meara AS, Kneuertz PJ, Presley CJ and Bridges JFP. Analysis of patient preferences in lung cancer - estimating acceptable tradeoffs between treatment benefit and side effects. Patient Prefer Adherence 2020; 14: 927-937.
[21] Zahoor I, Rui B, Khan J, Datta I and Giri S. An emerging potential of metabolomics in multiple sclerosis: a comprehensive overview. Cell Mol Life Sci 2021; 78: 3181-3203.
[22] Rochat B, Morsman JM, Murray GI, Figg WD and McLeod HL. Human CYP1B1 and anticancer agent metabolism: mechanism for tumor-specific drug inactivation? J Pharmacol Exp Ther 2001; 296: 537-541.
[23] Mayekar MK and Bivona TG. Current landscape of targeted therapy in lung cancer. Clin Pharmacol Ther 2017; 102: 757-764.
[24] Dockery LE, Tew WP, Ding K and Moore KN. Tolerance and toxicity of the PARP inhibitor olaparib in older women with epithelial ovarian cancer. Gynecol Oncol 2017; 147: 509-513.
[25] Wang SM, Ooi LL and Hui KM. Upregulation of Rac GTPase-activating protein 1 is significantly associated with the early recurrence of human hepatocellular carcinoma. Clin Cancer Res 2011; 17: 6040-6051.
[26] Zhang T, Wang C, Wang K, Liang Y, Liu T, Feng L and Yang X. RacGAP1 promotes the malignant progression of cervical cancer by regulating AP-1 via miR-192 and p-JNK. Cell Death Dis 2022; 13: 604.
[27] Kreider-Letterman G, Carr NM and Garcia-Mata R. Fixing the GAP: the role of RhoGAPs in cancer. Eur J Cell Biol 2022; 101: 151209.
[28] Ma L, Wang Z, Xie M, Quan Y, Zhu W, Yang F, Zhao C, Fan Y, Fang N, Jiang H, Wang Q, Wang S, Zhou J, Chen X and Shu Y. Silencing of cir-

cRACGAP1 sensitizes gastric cancer cells to apatinib via modulating autophagy by targeting miR-3657 and ATG7. Cell Death Dis 2020; 11: 169.

[29] Tian Q, Mu Q, Liu S, Huang K, Tang Y, Zhang P, Zhao J and Shu C. m6A-modified circASXL1 promotes proliferation and migration of ovarian cancer through the miR-320d/RACGAP1 axis. Carcinogenesis 2023; 44: 859-870.

[30] Perche O, Menuet A, Marcos M, Liu L, Pâris A, Utami KH, Kervran D, Cacheux V, Laudier B and Briault S. Combined deletion of two Condensin II system genes (NCAPG2 and MCPH1) in a case of severe microcephaly and mental deficiency. Eur J Med Genet 2013; 56: 635-641.

[31] Zhan P, Xi GM, Zhang B, Wu Y, Liu HB, Liu YF, Xu WJ, Zhu Q, Cai F, Zhou ZJ, Miu YY, Wang XX, Jin JJ, Li Q, Lv TF and Song Y. NCAPG2 promotes tumour proliferation by regulating G2/M phase and associates with poor prognosis in lung adenocarcinoma. J Cell Mol Med 2017; 21: 665-676.

[32] Kim JH, Shim J, Ji MJ, Jung Y, Bong SM, Jang YJ, Yoon EK, Lee SJ, Kim KG, Kim YH, Lee C, Lee BI and Kim KT. The condensin component NCAPG2 regulates microtubule-kinetochore attachment through recruitment of Polo-like kinase 1 to kinetochores. Nat Commun 2014; 5: 4588.

[33] Meng F, Zhang S, Song R, Liu Y, Wang J, Liang Y, Wang J, Han J, Song X, Lu Z, Yang G, Pan S, Li X, Liu Y, Zhou F, Wang Y, Cui Y, Zhang B, Ma K, Zhang C, Sun Y, Xin M and Liu L. NCAPG2 overexpression promotes hepatocellular carcinoma proliferation and metastasis through activating the STAT3 and NF-κB/miR-188-3p pathways. EBioMedicine 2019; 44: 237-249.

[34] Wu J, Li L, Jiang G, Zhan H, Zhu X and Yang W. NCAPG2 facilitates glioblastoma cells' malignancy and xenograft tumor growth via HBO1 activation by phosphorylation. Cell Tissue Res 2021; 383: 693-706.

[35] Xu T, Dong M, Wang Z, Li H and Li X. Elevated mRNA expression levels of NCAPG are associated with poor prognosis in ovarian cancer. Cancer Manag Res 2020; 12: 5773-5786.

[36] Jiang S, Huang J, He H, Liu Y, Liang L, Sun X, Li Y, Cong L, Qing B and Jiang Y. NCAPG2 maintains cancer stemness and promotes erlotinib resistance in lung adenocarcinoma. Cancers (Basel) 2022; 14: 4395.

[37] Pope BD, Ryba T, Dileep V, Yue F, Wu W, Denas O, Vera DL, Wang Y, Hansen RS, Canfield TK, Thurman RE, Cheng Y, Gülsoy G, Dennis JH, Snyder MP, Stamatoyannopoulos JA, Taylor J, Hardison RC, Kahveci T, Ren B and Gilbert DM. Topologically associating domains are stable units of replication-timing regulation. Nature 2014; 515: 402-405.

[38] Yeh CM, Sung WW, Lai HW, Hsieh MJ, Yen HH, Su TC, Chang WH, Chen CY, Ko JL and Chen CJ. Opposing prognostic roles of nuclear and cytoplasmic RACGAP1 expression in colorectal cancer patients. Hum Pathol 2016; 47: 45-51.

[39] Navaei ZN, Khalili-Tanha G, Zangouei AS, Abbaszadegan MR and Moghbeli M. PI3K/AKT signaling pathway as a critical regulator of Cisplatin response in tumor cells. Oncol Res 2021; 29: 235-250.